*Int. J. Electrochem. Sci.*, 16 **(2021)** Article ID: 210663, doi: 10.20964/2021.06.62

International Journal of
ELECTROCHEMICAL
SCIENCE
www.electrochemsci.org

# Pd-Al Alloys Formation by Aluminium Underpotential Deposition on Palladium from Equimolar $AlCl_3$+NaCl Melt

*Nataša M. Vukićević*[1*], *Vesna S. Cvetković*[1], *Niko Jovićević*[2], *Jovan N. Jovićević*[1]

[1] University of Belgrade-Institute of Chemistry, Technology and Metallurgy, Department of Electrochemistry, Njegoševa 12, 11000 Belgrade, Republic of Serbia
[2] S&R Company, Statesville, NC 28677, USA
[*]E-mail: vukicevic@ihtm.bg.ac.rs

*Received:* 7 March 2021 / *Accepted:* 21 April 2021 / *Published:* 30 April 2021

The possibility of electrochemical underpotential deposition of aluminium onto palladium from equimolar $AlCl_3$+NaCl melts at temperatures between 200 ° and 300 °C was investigated. Electrochemical techniques used were cyclic voltammetry, chronoamperometry, potentiodynamic polarization and open circuit measurements. The results were analyzed by SEM, EDX and XRD. It was found that aluminium deposits underpotentially onto palladium at around 0.200 V vs. Al from the chloroaluminate melt used. It was established that under the given conditions, Al underpotential deposition onto the palladium substrate can result in AlPd and $Al_3Pd_4$ alloy synthesis by solid-state interdiffusion. The surface alloys synthetized are well adhering, microcrystalline deposits, having highly developed surface area suitable for applications such as hydrogen purification filters.

**Keywords:** Aluminium alloys, electrodeposition, intermetallics, solid-state interdiffusion, X-ray diffraction (XRD)

## 1. INTRODUCTION

Surface alloys made of transition metals with aluminium are of particular interest, because of their proven potential in advanced magnetic, catalytic and electrochemical applications [1–4]. In addition, their use in medicine as biocompatible materials seems to be very promising [5].

Because of existing and future applications, interest in improved synthesis of palladium-aluminium alloys has increased in both fundamental and application fields [1]. Palladium (Pd) and aluminium (Al) are known to form several binary alloys having various crystallographic orientation [6] and component compositions [7,8], commanding specific, rare and very useful characteristics.

Ongoing research regarding implementation of binary Pd-Al alloys as hydrogen separation membrane material in so-called “hydrogen-based economy” has been receiving a great deal of attention

recently [9,10]. Palladium, in its pure form or alloyed with aluminium, has shown the ability to allow hydrogen diffusion through the metal lattice and, at the same time, a potential to enhance resistance to carbon monoxide (CO) poisoning [9–12]. For example, the surface of the Pd-Al intermetallic (pure palladium containing up to 0.1 at.% of aluminium) favors adsorption of hydrogen at the expense of carbon monoxide and is often used as a membrane material (a filter) in the production of ultrapure hydrogen [11,13]. Some of the methods that have been used in fabrication processes of Pd-Al alloys, contributing to the improvements of the properties intended for good hydrogen permeability, better reproducibility, enlarged resistance to CO poisoning and gratifying cost efficiency are: arc-melting of the pure components under argon, and sequential annealing [13–15], chemisorption followed by subsequent annealing [16–18]. DC magnetron sputtering [19] and ion-beam irradiation [20] are methods used to incorporate a thin film of Pd-Al alloys, into a porous support.

Meanwhile, Pd-Al alloys which exhibit reduction in magnetic susceptibility, found their way into medicine as biocompatible materials [5]. Fabricating medical devices from Pd-Al alloys with additives such as titanium, zirconium, niobium, offers the possibility aligning the device functionality to a specific application such as magnetic resonance imaging (MRI) compatibility, radiopacity and optimized strength [5,21]. Pd-Al alloys made of at least 75 at.% Pd, 3 to 20 at.% Al, and one or few more additives, allow achievement combination of both biocompatibility and ultra-low magnetic susceptibility properties [5] .

It has been found that the concentration of the elements participating in the Pd-Al alloy [13,14], and the way that the atoms are arranged in the surface alloy [1,19], are of the essence to their effectiveness. Thus, it is to be expected that any specific application will greatly depend on the ability to manipulate the development of the alloy composition and structure. Electrochemical deposition has been used successfully for tailored synthesis of advanced alloy materials, especially considering shape and size of the micro and nanostructured deposited materials can be conveniently controlled by the choice of parameters and regimes of electrolysis [22,23].

The initial stage of metal electrodeposition onto another metal is sometimes manifested as a development of a monolayer of the depositing metal on top of another metal at the potentials more positive than the equilibrium potential of the depositing metal, e.g. underpotential deposition (UPD) [24–31]. However, it should be recalled that due to interdiffusion between the underpotentially deposited atomic monolayer and the substrate during aluminium UPD from molten salts electrolytes, intermetallic solid-state reaction can produce aluminium alloys [26,29–35]. In addition, alloys obtained by electrodeposition very often exhibit chemical composition and crystal structure different from those obtained by classical procedures [31,36,37]. Varying the metallic substrate material and the conditions of aluminium UPD offers exciting new potential opportunities to add novel structures that may not be available today.

There are no reports available on the electrochemical deposition or UPD of aluminium onto palladium substrate from molten salts electrolytes. However, applying the hypothesis proposed by Kolb *et al*. [24,25], half of the work functions difference between the substrate metal ($\Phi_{Pd}$) and the deposited metal ($\Phi_{Al}$) is 0.5 eV which suggests that there is a possibility for aluminium UPD onto palladium. Consequently, our goal was to establish whether there is electrochemical underpotential deposition of aluminium onto palladium from equimolar $AlCl_3$+NaCl molten salts electrolyte at temperatures up to

300 °C. Our previous works on aluminium underpotential electrodeposition from the mentioned electrolyte onto some other metal substrates, Cd [26], V [28], Zr [29], Ag [30], Au [34], indicated the possibility of alloy formation as a result of Al UPD onto Pd as well. This would establish an effective way to form thermally stable aluminium-palladium surface alloys that could be potentially applied in filters for extra pure hydrogen.

## 2. EXPERIMENTAL

Electrochemical experiments were conducted at 200 °, 250 ° and 300 °C, in a three-electrode electrochemical cell constructed from Pyrex glass for work with melts. Experiments were performed under 99.99% argon atmosphere, using an EG&G PAR Potentiostat/Galvanostat, (Model 273A, Oak Ridge, TN, USA) controlled by Power Suite software (Princeton Applied Research, Oak Ridge, TN, USA). Temperature was controlled by an electronic thermostat with precision of ±1 °C.

Working electrodes (WE) were made of palladium (Pd, 99.99%, Sigma-Aldrich, USA) in the form of wire (ø = 1mm) for electrochemical measurements, and a planar plate (surface area = 0.5 $cm^2$) for longer time electrodeposition. As a reference electrode an aluminium rod (Al, ø = 0.3 cm, 99.999%, Alfa Products, Thiokol/Ventron division, USA) was used, and an Al plate (surface area = 7.5 $cm^2$) served as a counter electrode.

In this work, potentials of the (Pd) working electrodes were measured relative to the potential of aluminium (Al) reference electrode in the melt used under given conditions.

Prior to each experiment, the palladium cathode was etched in aqua regia, while the reference and counter aluminium electrodes were mechanically polished then etched in the solutions made of 50 vol.% HF + 15 vol.% $H_2O$ and conc. $NH_4OH$ + 5 vol.% $H_2O_2$. Thereafter, the electrodes were rinsed with deionized water, absolute ethyl alcohol and dried before use. Procedures used for the electrolyte-chloroaluminate molten salt preparation and melt pre-electrolysis, were identical to those described in our previous works [26,28,30].

Cyclic voltammetry (CV) experiments on the Pd WE conducted in the aluminium UPD range were as follows: starting from the potential, $E_i$, usually 0.050 to 0.100 V more negative than the open-circuit potential (OCP) of the Pd WE moving to a different cathodic end potential, $E_f$, (0.010 to 0.050 V positive to the equilibrium potential of Al) and then back to the starting potential. Additionally, within the same potential range, the scan was interrupted when the working potential reached the final cathodic value $E_f$, (0.050 to 0.150 V positive to the equilibrium aluminium potential) and held for a chosen period of time, before starting the return scan.

Controlled aluminium UPD at three used temperatures was always initiated 5 min, after insertion of the WE into the chloroaluminate melt in order to allow the system to move to thermal equilibrium. After the potentiostatic deposition at a constant Al UPD, the WE was taken out from the cell under potential in order to preserve deposited material or possible alloys formed. The melt residue was removed from the WE by washing of the electrode with absolute ethyl alcohol (Zorka-Pharma, Šabac, R. Serbia) and dried.

"Open circuit measurements" included holding the deposition potential of the palladium cathode at 0.050 to 0.020 V vs. Al for one hour, whereupon the applied potential was switched off and the open-circuit potential of the working electrode was recorded as a function of time.

To record potentiodynamic polarization curves for the palladium WE in an equimolar $AlCl_3$+NaCl melt at different temperatures, the cathode potential was scanned from the starting value, $E_i$ = 0.000 V, to the final value, $E_f$ = 0.900 V, with a scan rate of 1 mV $s^{-1}$.

Surface morphology and composition of the obtained deposits were analyzed by scanning electron microscope (SEM: JEOL, model JSM-5800, Tokyo, Japan), equipped with the instrumentation for energy dispersive X-ray spectroscopy EDS (EDX), (Oxford INCA 3.2, Abingdon, U.K.).

Phase analysis of the deposits on the Pd cathode was performed at room temperature by X-ray diffraction (XRD) on a Philips PW 1050 powder diffractometer (Philips, Delft, The Netherlands), which uses Ni filtered CuK radiation ($\lambda$ = 1.54178 Å), scintillation detector within 20-80° 2$\theta$ range in steps of 0.05°, at a scanning time of 5 s per step.

## 3. RESULTS

Cyclic voltammograms recorded on palladium working electrode in the used electrolyte at three different temperatures (200 °, 250 ° and 300 °C) are presented in Fig. 1.

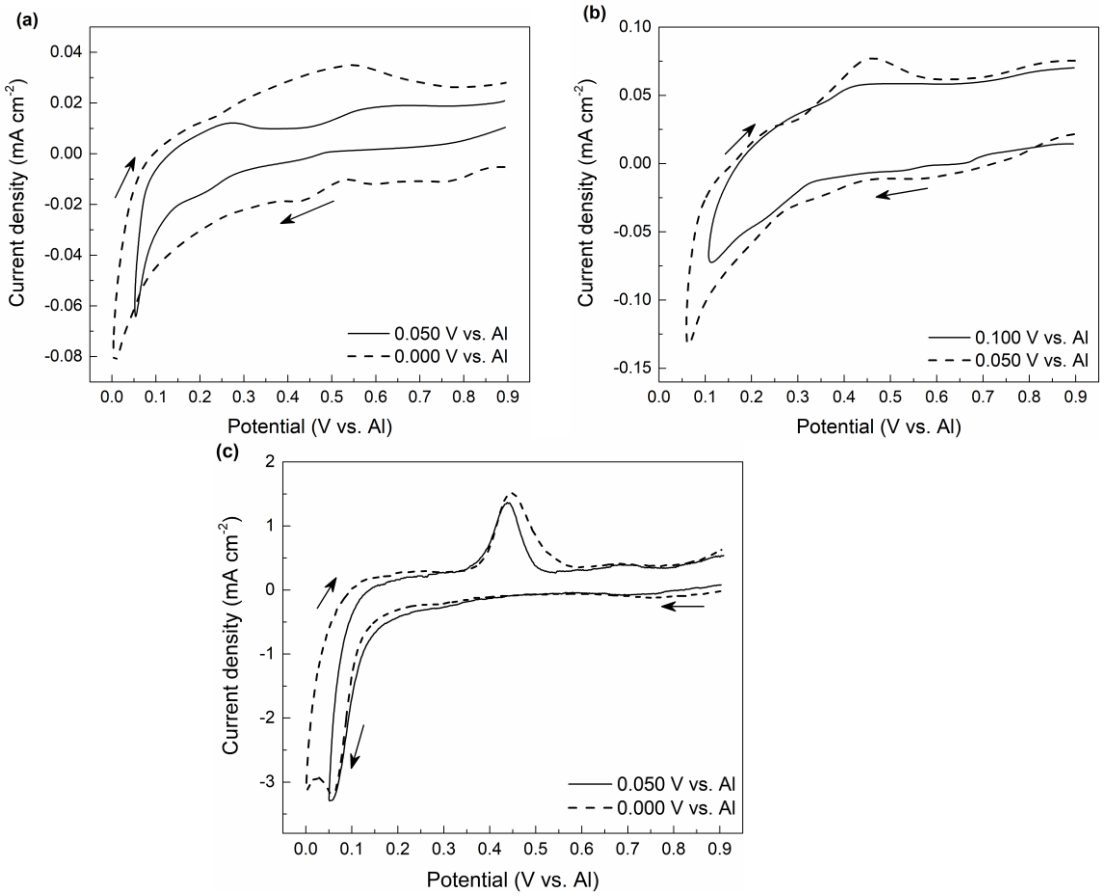


**Figure 1.** Voltammograms obtained with palladium working electrode in equimolar $AlCl_3$+NaCl electrolyte; ν = 10 mV $s^{-1}$: a) T = 200 °C, b) T = 250 °C, c) T = 300 °C.

Anodic current waves became better defined when the final cathodic potential, $E_f$, was held for a specific period of time before being allowed to return to the initial potential, $E_i$, Fig. 2.

The change in the "open circuit" working electrode potential as a function of time after 60 minutes of constant potential of 0.020 V vs. Al applied at 250 °C and 300 °C in the used electrolyte is presented in Fig. 3. Two shoulders were recorded. These two plateaux approximating constant potentials indicate the presence of two phases at the potentials between the equilibrium potentials of aluminium and palladium in the used electrolyte.

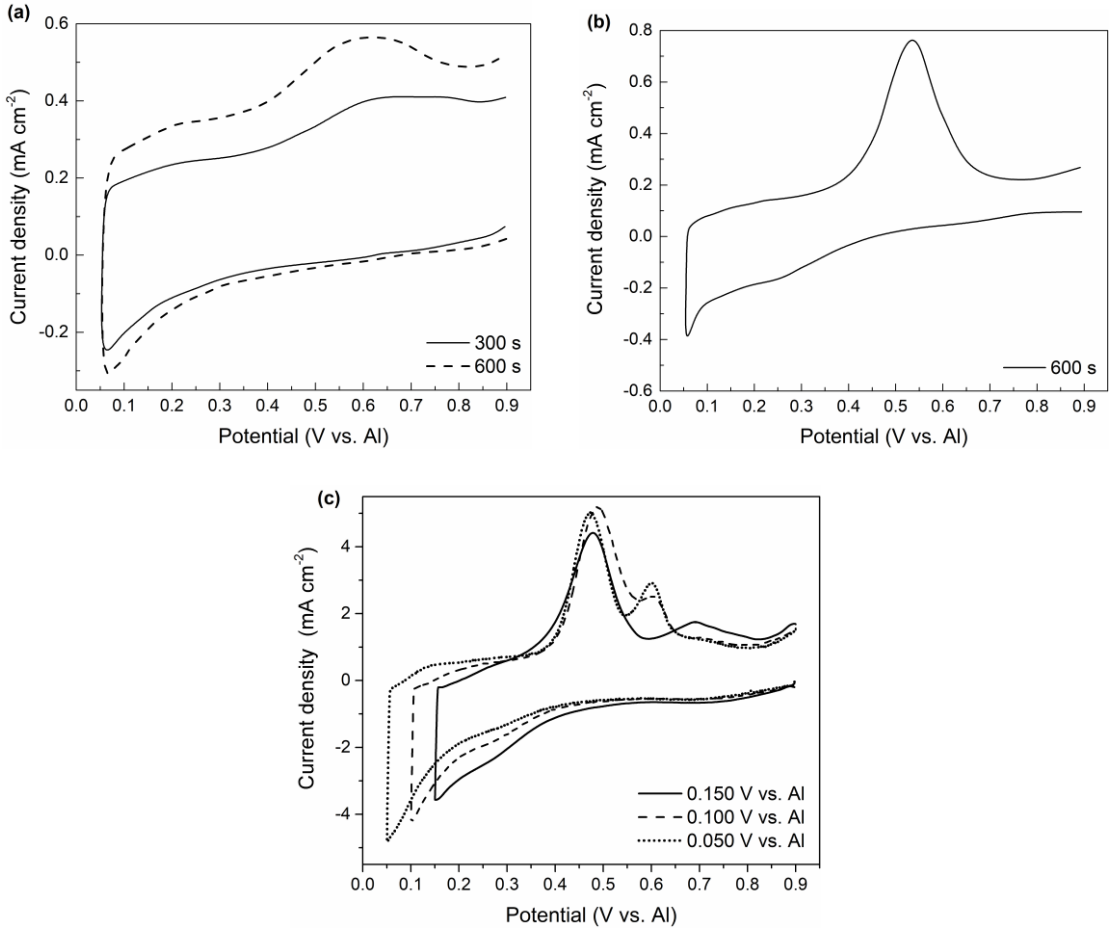


**Figure 2.** Voltammograms obtained with palladium working electrode in equimolar $AlCl_3$+NaCl electrolyte, $\nu = 10$ mV $s^{-1}$: a) T = 200 °C, potential change sequence $E_i = 0.900$ V → $E_f = 0.050$ V vs. Al, b) T = 250 °C, potential change sequence $E_i = 0.900$ V → $E_f = 0.050$ V vs. Al, c) T = 300 °C, potential change sequence $E_i = 0.900$ V → different cathodic end potential $E_f$, $E_f$ holding time 600s.

Potentiodynamic polarization curves recorded in the potential range between 0.000 V and 0.900 V vs. Al with the Pd WE in the used electrolyte at three different temperatures (see Fig. 4) showed two equilibrium potentials $E_I$ and $E_{II}$. The values did not change significantly with increasing temperature, and were close to the potentials calculated as mid-point values between cathodic and anodic current peaks in Figs. 1 and 2, and the shoulders recorded in Fig. 3. These potentials ($E_I$ and $E_{II}$, Fig. 4) should indicate the phases in equilibrium with aluminium ions present in the used electrolyte. Being positive to the aluminium equilibrium potential in the used electrolyte and in the same time negative to the

palladium equilibrium potential (≈1.025V vs. Al) in the same electrolyte, they should reflect two phases formed as the result of aluminium underpotential deposition onto palladium working electrode.

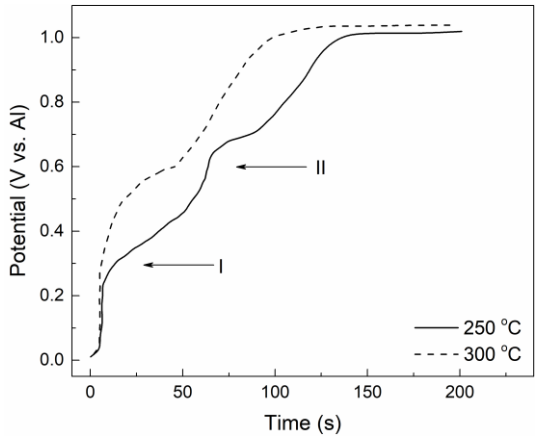


**Figure 3.** Open circuit potentiograms for a Pd WE after Al UPD at the potential of 0.020 V vs. Al for 60 min. at 250 °C and 300 °C.

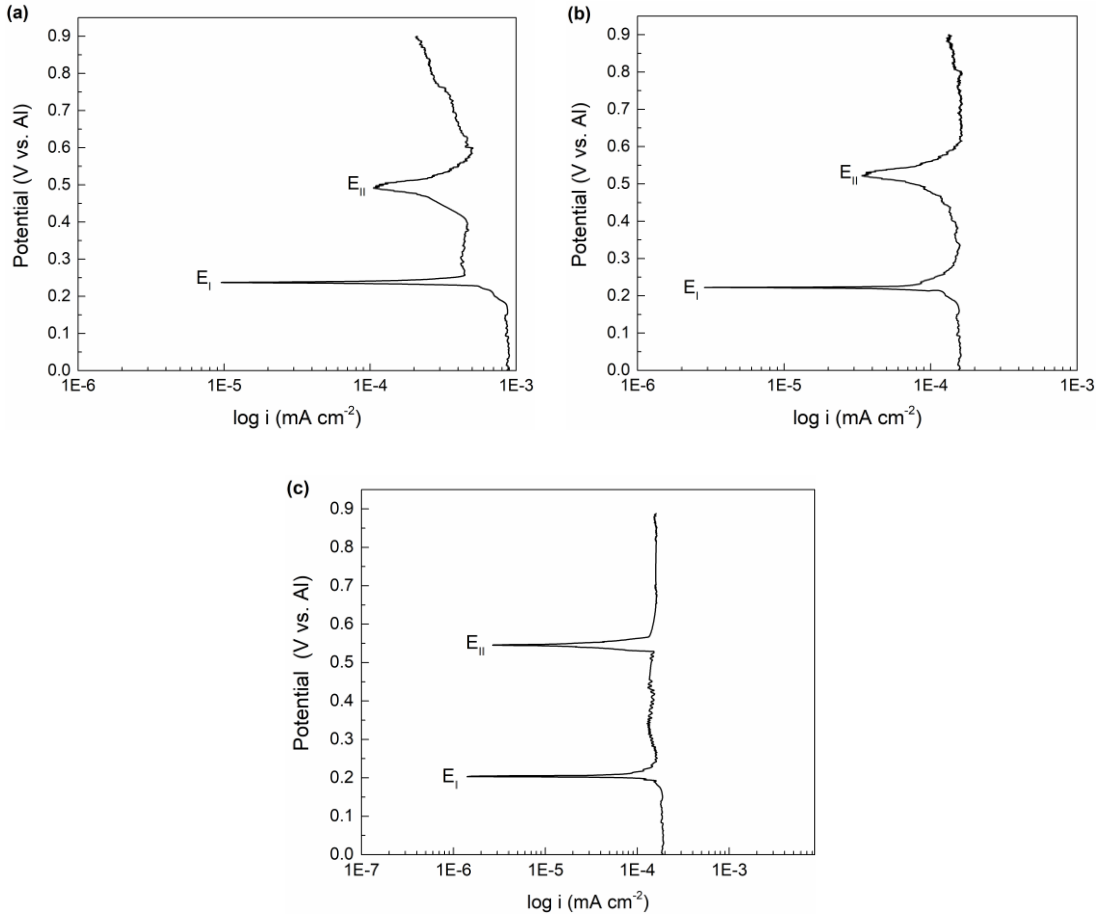


**Figure 4.** Potentiodynamic polarization curves on the palladium working electrode in equimolar $AlCl_3$+NaCl electrolyte; ν = 1 mV $s^{-1}$; potential sequence $E_i$ = 0.000 V → 0.900 V vs. Al at: a) T = 200 °C, b) T = 250 °C, c) T = 300 °C.

The results obtained by the SEM and EDS analysis of the palladium electrode surface exposed for 2 hours to a constant underpotential of 0.050 V vs. Al in used electrolyte at 250 °C are presented in Figs. 5-6.

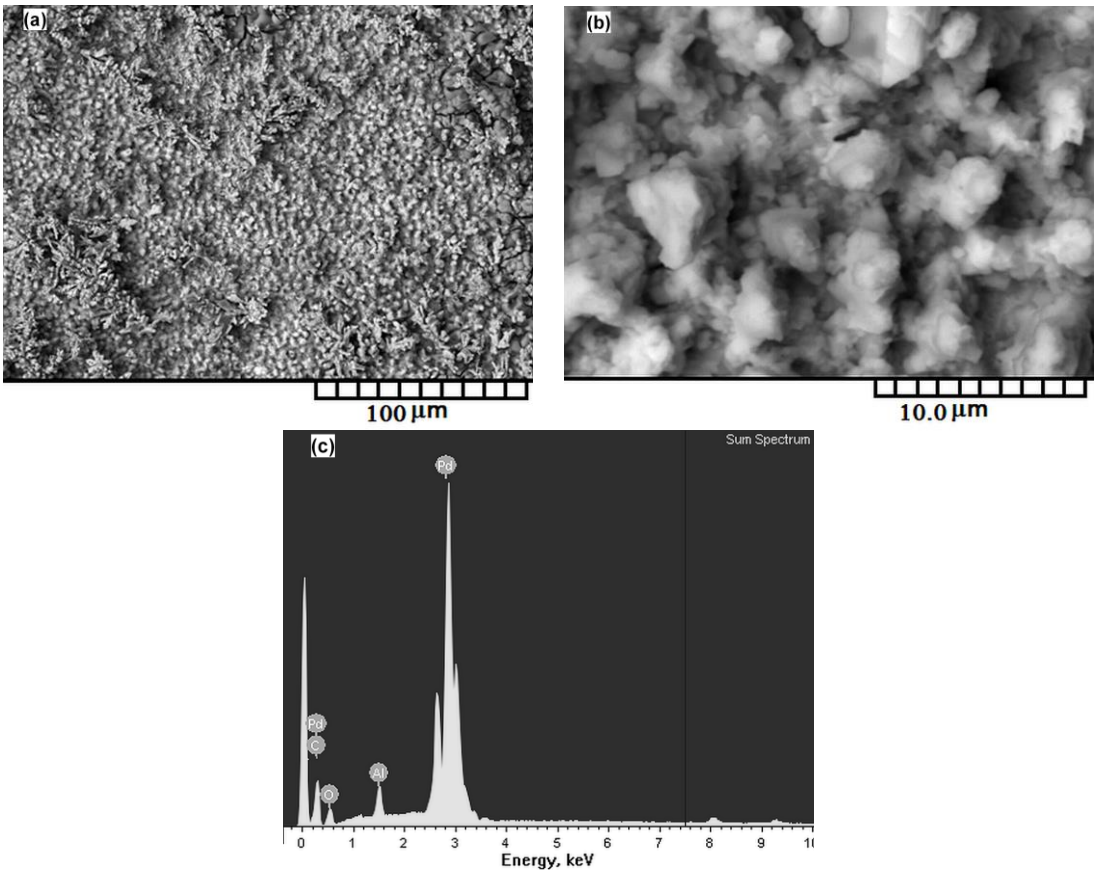


**Figure 5.** SEM micrographs at: a) lower, b) higher magnification, and c) EDS analysis, of the Pd surface after 2 hours of Al UPD at 0.050 V vs. Al in the used electrolyte at 250 °C.

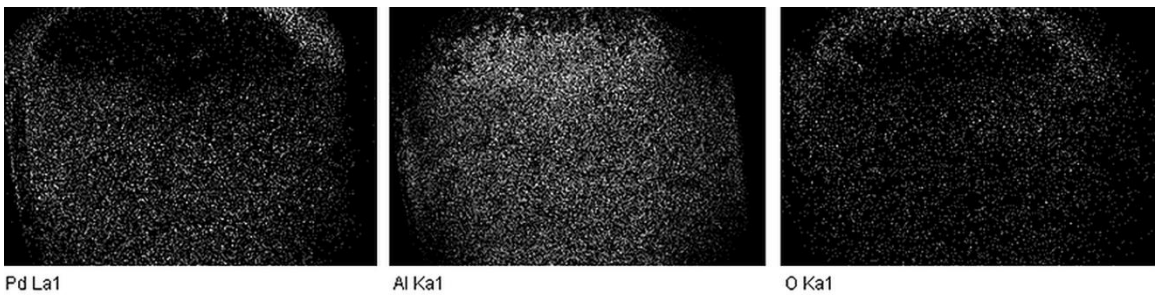


**Figure 6.** EDX maps of palladium, aluminium and oxygen distribution after 2 hours of Al UPD onto palladium substrate, at 250 °C; the same surface presented in Fig. 5.

SEM revealed well developed surface of a crystalline deposit, well adhered to the substrate surface Fig. 5a and b. Higher magnification images of the resulting deposit showed nodular agglomerations which are closely packed and continuously cover the entire working surface.

According to semi-quantitative EDS measurements, Fig. 5c the content of Al and Pd in the resulting deposit was 4.07 at.% and 43.57 at.%, respectively. There was also oxygen recorded, which should be attributed to exposure during the sample handling. The white areas, Fig. 6, in the EDX maps of the sample from Fig. 5a and b, has given us a clear picture of position and distribution of Pd, Al and O in the deposit.

These data definitely identify aluminium as electrodeposited from the used electrolyte onto palladium electrode at potentials more positive than the equilibrium potential of aluminium at temperatures applied. When the final cathodic potential, $E_f$, was made more negative (for example 0.020 or 0.010 V vs. Al), under other conditions kept the same, UPD aluminium amounts in the palladium substrate increased even if the deposition time was made shorter.

XRD analysis on the corresponding electrodes confirmed that underpotentially deposited aluminium onto palladium produces Pd-Al alloys. Diffractograms in Figs. 7-9 revealed which Pd-Al alloys were synthetized.

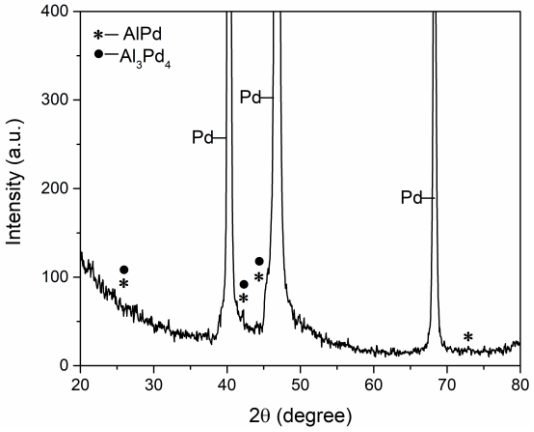


**Figure 7.** XRD analysis of the Pd electrode surface after 5 hours of Al deposition under potentiostatic regime applied at 0.200 V vs. Al, T = 250 °C; (*)- AlPd; (●)- $Al_3Pd_4$.

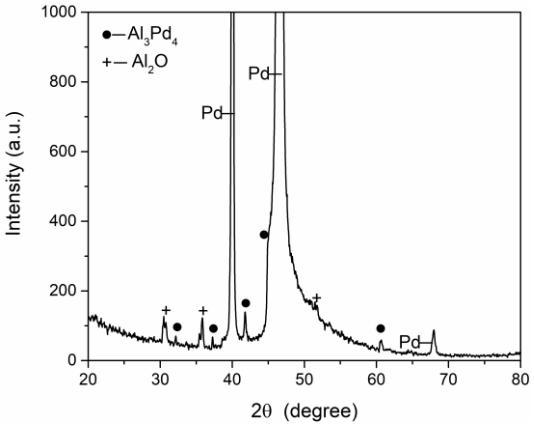


**Figure 8.** XRD analysis of the Pd electrode surface after 5 hours of Al deposition under potentiostatic regime applied at 0.100 V vs. Al, T = 250 °C; (●)- $Al_3Pd_4$; (+)- $Al_2O$.

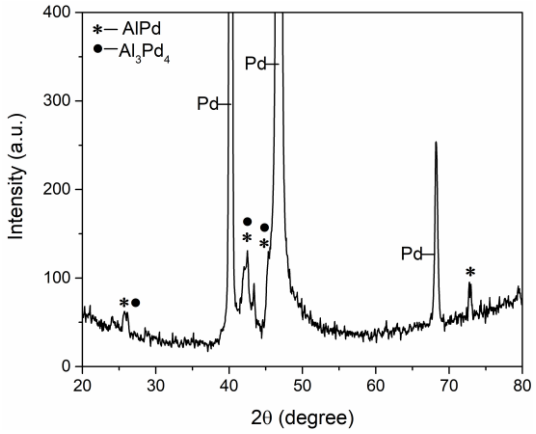


**Figure 9.** XRD analysis of the Pd electrode surface after 5 hours of Al deposition under potentiostatic regime applied at 0.050 V vs. Al, T = 250 °C; (*)- AlPd; (●)- $Al_3Pd_4$.

## 4. DISCUSSION

Cyclic voltammograms revealed that negative current densities of the voltammograms did not produce pronounced waves, while anodic current waves were well defined. Articulation of the cathodic and anodic current waves in the aluminium underpotential range (the potentials positive to the aluminium equilibrium potential in the used system) was more pronounced with increased temperature. At 300 °C both cathodic and anodic current waves were well defined, indicating that processes of electrodeposition and dissolution were taking part on the palladium WE in the used electrolyte in the area of aluminium underpotentials, Fig. 1.

By increasing the holding time at $E_f$, at a constant temperature in the aluminium UPD range, anodic current densities increased, making the charge encompassed by the anodic current wave larger. The increased anodic charge indicates increased amounts of the previously electrodeposited aluminium being dissolved, Fig. 2.

**Table 1.** Cathodic end holding potential, E (V vs. Al) and corresponding dissolution charge (mAs $cm^{-2}$) in the anodic section of the voltammograms on palladium electrodes as a function of deposition holding time τ (s) and temperature T (ºC).

| ***Electrode*** | ***Holding time [s]*** | ***E [V vs. Al]*** | ***Dissolution charge [mAs $cm^{-2}$]*** | | |
|---|---|---|---|---|---|
| | | | ***200 °C*** | ***250 °C*** | ***300 °C*** |
| **Pd** | 60 | 0.050 | 2.1 | 3.2 | 16 |
| | 300 | 0.050 | 9.5 | 14.1 | 81 |
| | 600 | 0.050 | 11.3 | 19.2 | 182 |

Amounts of the charge encompassed by the cathodic and anodic current waves calculated from the voltammograms recorded on palladium working electrode exposed to aluminium underpotential

deposition and dissolution are substantially larger than the charge needed for the electrodeposition of a close packed Al(111) monolayer, which is 1.17 mAs $cm^{-2}$ [26,30]. When deposition time at the cathodic end potential (holding time) was made longer, the cathodic currents would not increase, while the corresponding anodic current wave maxima and dissolution charges increased, Table 1.

However, increasing the system temperature, all other conditions being the same, provoked an increase of the peak currents and increase of the charge within the limits of the current waves. This indicated that underpotential deposition of aluminium onto palladium does not end with one Al monolayer being formed on the Pd surface, but that additional amounts of aluminium were deposited. Aluminium underpotentially deposited in excess of one monolayer could make alloys with palladium substrate by interdiffusion processes [26,27,30,31]. This would result in a development of at least one new phase, in addition to the underpotentially deposited Al monolayer. These new phases should have their own equilibrium potentials in contact with the electrolyte used. The current wave potentials recorded on the voltammograms were in agreement with this proposition: there was one cathodic and two anodic current peaks, Table 2. The "open circuit measurements", Fig. 3, also revealed two discrete "shoulders", I and II, thus defining equilibrium potentials of at least two phases made during Al underpotential deposition onto Pd substrate under given conditions, Table 3.

**Table 2.** Peak potential values, E (V vs. Al) of the cathodic and anodic current waves obtained by CV in Al UPD range onto Pd at different temperatures from equimolar $AlCl_3$+NaCl melt.

| ***Electrode*** | ***E [V vs. Al]*** | ***200 °C*** | ***250 °C*** | ***300 °C*** |
|---|---|---|---|---|
| **Pd** | Cathodic | 0.203 | 0.176 | 0.101 |
| | Anodic I | 0.279 | 0.446 | 0.446 |
| | Anodic II | 0.633 | 0.611 | 0.567 |

Prolonged potentiostatic aluminium underpotential deposition led to a proportional increase in time needed for the dissolution of the phases during the "open circuit measurements", but had very little or no influence on the values of the plateaux potentials.

**Table 3.** Inflection points potentials, (V vs. Al) obtained in "open circuit" measurements after one hour of aluminium UPD at 0.020 V vs. Al on palladium in equimolar $AlCl_3$+NaCl melt for different temperatures T (ºC).

| ***Electrode*** | ***Inflection point potential [V vs. Al]*** | ***200 °C*** | ***250 °C*** | ***300 °C*** |
|---|---|---|---|---|
| **Pd** | I | - | 0.233 | 0.314 |
| | II | - | 0.499 | 0.514 |

Values of the two plateaux (equilibrium) potentials recorded were comparable to the values of the two anodic current waves potentials from Table 2 obtained from CV experiments.

Potentiodynamic polarization curves, Fig. 4, recorded in the Al underpotential range also show two equilibrium potentials ($E_I$ and $E_{II}$) at values very close to those seen in the "open circuit measurements" done under the same conditions. Actually, the $E_I$ value changed from 0.240 V to 0.225 V and finally to 0.200 V vs. Al while $E_{II}$ value changed from 0.494 V to 0.526 V and finally to 0.545 V vs. Al when the working temperature changed from 200 ° to 250 ° and to 300 °C, which was a significant agreement in the recorded values as well as in dependence on the temperature between the equilibrium potentials of the two phases presented in Fig. 3 and Fig. 4. This is characteristics for the potential of the solid phase in equilibrium with its ions in the surrounding electrolyte.

It appeared that electrodeposition of aluminium in the underpotential region onto palladium proceeded after at least one complete monolayer formed with the same rate with which aluminium atoms from the monolayer keep entering solid-state intermetallic reactions with the substrate. It seemed that this dynamic quasi-equilibrium persists during the solid-state intermetallic reaction, most probably, due to solid-state interdiffusion with the substrate.

This led to the conclusion that electrochemical measurements indicate at least two Pd-Al alloys being formed during Al underpotential deposition onto Pd substrate from equimolar $AlCl_3$+NaCl mixture at 200 °, 250 ° and 300 °C. EDS analysis of the palladium surface after Al underpotential deposition done at all three temperatures registered aluminium on/in the surface, Figs. 5 and 6.

According to XRD analysis surface aluminium-palladium alloys were synthetized even at potentials as positive to the aluminium equilibrium potential as 0.100 and 0.200 V vs. Al (Figs. 7 and 8). For example, XRD analysis of the Pd electrode kept for 5 hours at 0.200 V vs. Al and 250 °C (Fig. 7), has shown that Al UPD at this potential offers indications of Pd-Al alloys being formed.

Results of our XRD analysis, examples given in Figs. 7-9, clearly indicate AlPd and $Al_3Pd_4$ intermetallic compounds formed by aluminium underpotential deposition onto palladium from equimolar $AlCl_3$+NaCl melt at 250 °C:

- cubic AlPd (most intensive peaks in diffractogram are at $2\theta$ values of 25.89; 36.93; 41.48; 45.65; 60.11 and 72.68 degrees [JCPDS No. 00-029-0065];
- cubic $Al_3Pd_4$ (most intensive peaks in diffractogram are at $2\theta$ values of 26.15; 41.9 and 46.13 degrees [JCPDS No. 00-029-0066].

Analysis of all the diffractograms obtained has shown that aluminium underpotential deposition onto palladium, at temperatures between 200 ° and 300 °C, always produced several alloys which possessed characteristic $2\theta$ values very close to those of the substrate, which made their matching to the $2\theta$ values listed in the literature difficult.

The Al-Pd phase diagram, which has not yet been precisely finalized, envisages nine intermetallic phases none of which can be formed at temperatures below 600 °C [6–8]. Those richer in palladium are: $Al_2Pd_5$, $AlPd_2$, $Al_3Pd_5$, AlPd and $Al_3Pd_2$. First three in the listing containing between 71.7 at.% and 62.5 at.% of Pd exhibit an orthorhombic structure, and last few containing between 56 at.% and 39.41 at.% show a cubic structure. Some authors, however, found that characteristics of Al-Pd phases, AlPd, $AlPd_2$ and $Al_2Pd_5$ are those of nonstoichiometric intermetallic compounds [38]. Others have produced amorphous thin layer phases by cooling, which when thicker became cubic metastable phase of $Al_2Pd$

stoichiometry [39,40]. Some have used vapour deposition to nucleate Al-Pd phases of different structures [41]. It should be mentioned that maximum aluminium dissolution in palladium is 20 at.% and that at 1055 °C. In other words, the alloys (AlPd, $Al_3Pd_4$) recorded in the analysis made on the deposits formed during the Al UPD onto Pd (and illustrated by Figs. 7-9) at temperatures applied (200 °, 250 ° and 300 °C) should not have been synthetized.

Available literature shows examples of Al UPD from melts on a number of metals resulting in examples of alloys being formed at temperatures below those predicted by the phase diagrams of the individual pairs [26,29–35]. Solid-state interdiffusion between atoms of the deposited metal and the substrate metal is mainly responsible for the alloy formation at the temperatures, sometimes well below those demanded by the phase diagram [26,27,30,31,42,43].

To the best of our knowledge, there are no reports regarding electrochemical overpotential and underpotential deposition of aluminium onto palladium from melts. There are only a few reports of electrodeposition from ionic liquids [44]. However, there is a number of reports on ion scattering [16,45] and vacuum deposition of aluminium onto palladium [1,16–18,20,46]. Discussing the results, the authors propose formation of AlPd, $Al_3Pd$ and $Al_4Pd$ as possible phases with primitive cubic (the cell of 2 atoms), hexagonal (a = 1.30 nm, c = 0.96 nm) and orthorhombic structures (a = 2.2505 nm, b = 1.7729 nm and c = 1.184 nm), respectively. They also proposed a mechanism of surface Al-Pd alloys formation induced by Al scattering and chemisorbed deposition onto Pd in three steps [1,16–18,20]:

- Al atoms are chemisorbed onto Pd single-crystal plane making a coverage from a half to a full Al monolayer;
- during annealing at the temperatures from 175 ° to 225 °C starts a stoichiometric substitution of an adsorbed Al atom with a Pd atom from the Pd substrate until Al coverage is as low as $\Theta \approx 0.5$ of an Al-Pd alloy monolayer [47]; the process continues by further Al atoms migration into the bulk Pd exchanging places with Pd atoms which come out to the immediate Al layer above and react with Al atoms remaining as second surface Al-Pd alloy layer; thus a bi-layer is formed made of Al-Pd surface alloy;
- when bi-layer coverage exceeds $\Theta \approx 0.5$ nucleation of 2D bi-layer islands starts, some of the round shape and some of a rough shape.

With time or temperature increases, 2D islands can become 3D islands providing that Al atoms are continuously supplied. It was mentioned that only ~ 22 at.% of deposited aluminium atoms were used for formation of the surface alloy [17]. The last two layers, over underlayers of Al-Pd alloy formed on Pd substrate, are always a layer of Pd(2x2)p4g on top of a layer of c(2x2)Al-Pd alloy. This model suggested that the alloy formed should be an $AlPd_3$ composition, however, this was not confirmed [18].

It is possible that this or some other modified form of this model takes part in the formation of the alloys observed during Al UPD onto Pd from the equimolar $AlCl_3$+NaCl melt at temperatures 200 °, 250 ° and 300 °C. It should be noted that SEM photographs of the Pd-Al alloy islands-deposit, Fig. 5, are similar in appearance to those reported in the work describing Pd-Al alloy formation by Al chemisorption and annealing on Pd [17].

## 5. CONCLUSIONS

This report is the first in the available literature on the aluminium underpotential deposition onto palladium from inorganic melts ($AlCl_3$+NaCl) at temperatures below 300 °C.

Solid-state interdiffusion processes involving underpotentially deposited aluminium and substrate palladium atoms take part during deposition and result in surface alloys formation. Recorded alloys, AlPd and $Al_3Pd_4$, were synthetized at temperatures below 300 °C, which are several hundred degrees Celsius lower than the temperatures defined by the Pd-Al phase diagram.

These results could be a basis for a new and less complicated technology for production of filters to be used in safeguarding hydrogen by decreasing the poisoning effect of carbon monoxide.

ACKNOWLEDGEMENT
V.S.C. and N.M.V. acknowledge the financial support for the investigation received from the Ministry of Education, Science and Technological Development of the Republic of Serbia (Grant No. 451-03-9/2021-14/200026).

## References

1. J.E. Kirsch, C.J. Tainter, *Surf. Sci.*, 602 (2008) 943.
2. V. Shutthanandan, A.A. Saleh, N.R. Shivaparan, R.J. Smith, *Surf. Sci.*, 350 (1996) 11.
3. M. Palcut, L. Ďuriška, M. Špoták, M. Vrbovský, Gerhátová, I. Černičková, J. Janovec, *J. Min. Metall. Sect. B Metall.*, 53 (2017) 333.
4. J.-J. Dong, L. Fan, H.-B. Zhang, L.-K. Xu, L.-L. Xue, *Acta Metall. Sin. (English Lett.)*, 33 (2020) 595.
5. A.S. Klein, I. Smith, E. F., P. Hale, Palladium-Based Alloys for Use in the Body and Suitable for MRI Imaginig, WO2009097221, 2009.
6. A.J. Mcalister, *Bull. Alloy Phase Diagrams*, 7 (1986) 368.
7. M. Yurechko, A. Fattah, T. Velikanova, B. Grushko, *J. Alloys Compd.*, 329 (2001) 173.
8. H. Okamoto, *J. Phase Equilibria Diffus.*, 29 (2008) 199.
9. D. Alique, D. Martinez-Diaz, R. Sanz, J. Calles, *Membranes (Basel).*, 8 (2018) 5.
10. M.R. Rahimpour, F. Samimi, A. Babapoor, T. Tohidian, S. Mohebi, *Chem. Eng. Process. Process Intensif.*, 121 (2017) 24.
11. J.J. Conde, M. Maroño, J.M. Sánchez-Hervás, *Sep. Purif. Rev.*, 46 (2017) 152.
12. M. Lukaszewski, M. Soszko, A. Czerwiński, *Int. J. Electrochem. Sci.*, 11 (2016) 4442.
13. D. Wang, T.B. Flanagan, K.L. Shanahan, *J. Memb. Sci.*, 253 (2005) 165.
14. D. Wang, H. Noh, S. Luo, T.B. Flanagan, J.D. Clewley, R. Balasubramaniam, *J. Alloys Compd.*, 339 (2002) 76.
15. D. Wang, T.B. Flanagan, R. Balasubramaniam, *J. Alloys Compd.*, 364 (2004) 105.
16. D.J. O'Connor, Y.G. Shen, J. Yao, *Nucl. Instruments Methods Phys. Res. Sect. B Beam Interact. with Mater. Atoms*, 135 (1998) 355.
17. K. Kishi, A. Oka, N. Takagi, M. Nishijima, T. Aruga, *Surf. Sci.*, 460 (2000) 264.
18. T. Aruga, K. Kishi, M. Nishijima, *Surf. Sci.*, 493 (2001) 325.
19. P. Dayal, N. Savvides, M. Hoffman, *Thin Solid Films*, 517 (2009) 3698.
20. L.S. Hung, M. Nastasi, J. Gyulai, J.W. Mayer, *Appl. Phys. Lett.*, 42 (1983) 672.
21. J.C. Wataha, K. Shor, *Expert Rev. Med. Devices*, 7 (2010) 489.
22. A.R. Despić, V.D. Jović, R.E. White (Ed.), Mod. Asp. Electrochem., Plenum Press, (1995) New

York, pp. 143–232.
23. V.D. Jović, U.Č. Lačnjevac, B.M. Jović, S. Djokić (Ed.), Electrodepos. Surf. Finish. Mod. Asp. Electrochem., Springer, New York, NY, (2014), pp. 1–84.
24. D.M. Kolb, H. Gerischer, *Surf. Sci.*, 51 (1975) 323.
25. D.M. Kolb, M. Przasnyski, H. Gerischer, *Electroanal. Chemtstry Interfacial Electrochem.*, 54 (1974) 25.
26. N. Jovićević, V.S. Cvetković, Ž.J. Kamberović, J.N. Jovićević, *Metall. Mater. Trans. B Process Metall. Mater. Process. Sci.*, 44 (2013) 106.
27. N. Jovićević, V.S. Cvetković, Ž.J. Kamberović, J.N. Jovićević, *Int. J. Electrochem. Sci.*, 7 (2012) 10380.
28. N. Jovićević, V.S. Cvetković, Ž. Kamberović, T.S. Barudžija, *Int. J. Electrochem. Sci.*, 10 (2015) 8959.
29. V. Cvetković, N. Jovićević, N. Vukićević, J. Jovićević, *J. Serbian Chem. Soc.*, 84 (2019) 1329.
30. B. Radović, R.A.H. Edwards, V.S. Cvetković, J.N. Jovićević, *Kov. Mater.*, 48 (2010) 55.
31. V.S. Cvetković, N.M. Vukićević, J.N. Jovićević, J.S. Stevanović (Ed.), Met. Met. Electrocatal. Mater. Altern. Energy Sources Electron., Nova Science Publisher, Inc, (2019) New York, pp. 371–423.
32. G.R. Stafford, C.L. Hussey, R.C. Alkire, D.M. Kolb (Eds.), Adv. Electrochem. Sci. Eng., Wiley-VCH Verlag GmbH, New York, (2001) Weinheim, pp. 275–348.
33. O.A. Oveido, L. Reinaudi, S.G. Garcia, E.P.M. Levia, Underpotential Deposition: From Fundamentals and Theory to Aplications at the Nanoscale, Springer International Publishing Switzerland, (2016).
34. B.S. Radović, R.A.H. Edwards, J.N. Jovićević, *J. Electroanal. Chem.*, 428 (1997) 113.
35. N.M. Vukićević, V.S. Cvetković, L.S. Jovanović, S.I. Stevanović, J.N. Jovićević, *Int. J. Electrochem. Sci.*, 12 (2017) 1075.
36. W. Plieth, *Surf. Coatings Technol.*, 169–170 (2003) 96.
37. P.L. Cavallotti, L. Nobili, A. Vicenzo, *Electrochim. Acta*, 50 (2005) 4557.
38. M. Li, C. Li, F. Wang, W. Zhang, *Intermetallics*, 14 (2006) 39.
39. M. Ellner, U. Kattner, B. Predel, *J. Less Common Met.*, 87 (1982) 117.
40. G.V.. Sastry, C. Suryanarayana, *Mater. Sci. Eng.*, 47 (1981) 193.
41. G.V.S. Sastry, C. Suryanarayana, G. van Tendeloo, *Phys. Status Solidi*, 73 (1982) 267.
42. R. Vidu, S. Hara, *Surf. Sci.*, 452 (2000) 229.
43. R. Vidu, S. Hara, *J. Electroanal. Chem.*, 475 (1999) 171.
44. F. Endres, D. MacFarlane, A.P. Abbott, eds., Electrodeposition from Ionic Liquids, WILEY-VCH Verlag GmbH, (2008) Weinheim.
45. Y.G. Shen, J. Yao, D.J. O'Connor, B. V. King, R.J. MacDonald, *Phys. Rev. B*, 56 (1997) 9894.
46. M. Ellner, U. Kattner, B. Predel, *J. Appl. Crystallogr.*, 14 (1981) 212.
47. W.W. Pai, A.K. Swan, Z. Zhang, J.F. Wendelken, *Phys. Rev. Lett.*, 79 (1997) 3210.